JOURNAL OF PROPULSION AND POWER
Vol. 18, No. 4, July–August 2002

Radiometric Analysis from the 26-Kilowatt Electric Propulsion Space Experiment Flight

G. G. Spanjers*
U.S. Air Force Research Laboratory, Edwards Air Force Base, California 93524
J. H. Schilling†
Sparta, Inc., Edwards Air Force Base, California 93524
D. R. Bromaghim‡
U.S. Air Force Research Laboratory, Edwards Air Force Base, California 93524
and
L. K. Johnson§
The Aerospace Corporation, El Segundo, California 90245

The U.S. Air Force Research Laboratory's Electric Propulsion Space Experiment (ESEX) was launched and operated in early 1999 to demonstrate the compatibility and readiness of a 30-kW class ammonia arcjet for satellite propulsion applications. As part of this flight, an array of onboard contamination sensors was used to assess the effect of the arcjet and other environments on the spacecraft. The sensors consisted of microbalances to measure material deposition, radiometers to assess material degradation due to thermal radiation or contamination, and solar cell segments to investigate solar array degradation. Over eight firings of the ESEX arcjet, and 33 min, 26 s operating time, the radiometer near the thruster, viewing the arcjet plume and body, experiences a change in the thermal properties of its coating from the firings. Radiometers with no view of the arcjet, or a view of only the plume, show no change. In general, degradation effects are observed only on sensors near the thruster exhaust nozzle, a location unlikely to be used in an operational high-power electric propulsion system. No degradation effects are observed in the backplane of the thruster. For future programs, although engineering measures may be needed for spacecraft equipment in the immediate vicinity of the thruster body, the arcjet environment is generally benign.

Nomenclature

A	=	area, m^2
C_P	=	specific heat, J/kg
k	=	thermal conductivity, W/m · K
m	=	mass, kg
$\dot{Q}_{\text{in}}$	=	heat flux into sensor, W
$\dot{Q}_{\text{rad}}$	=	radiative heat flux, W
$\dot{Q}_T$	=	heat flux conducted down radiometer stem, W
$\dot{Q}_{12}$	=	radiative heat within radiometer body, W
T	=	temperature, K

I. Introduction

SPACECRAFT thermal control surfaces can be degraded by excessive heat flux, which can alter the emissive and absorptive properties of spacecraft materials, thereby changing the thermal balance of the satellite. Understanding the coupling of these effects with high-power electric propulsion is of critical importance to the development of next-generation large U.S. Air Force (USAF) space structures. A major goal of the USAF Electric Propulsion Space Experiment (ESEX)[1] is to explore these issues by measuring the contamination effects of a 30-kW class arcjet in flight. ESEX was launched on 23 February 1999 as one of nine experiments aboard the USAF's Advanced Research and Global Observation Satellite (ARGOS).[2]

An array of sensors is positioned at strategic locations of the ESEX package to assess the contamination effects. Thermal surface degradation due to the arcjet firing is measured using four radiometers. These radiometers are coated with S13-GLO white paint, a common thermal surface material with low solar absorptivity and high emissivity. Measurement of heat transfer through the coating determines the degradation of S13-GLO when subjected to the spectral emission of the high-power arcjet. This degradation impacts the thermal design of spacecraft using high-power electric propulsion. Mass deposition is measured using four thermoelectric quartz crystal microbalances (TQCMs).[3] A sample gallium–arsenide (GaAs) solar array segment placed near the arcjet nozzle determines impact on the satellite power-generation capability.[4] Electromagnetic interference is characterized using a set of onboard antennas and ground stations.[5] This paper focuses on heat flux and material degradation measurements from the radiometers. Measurements from the other onboard sensors may be found in companion papers[3–5] within this issue.

During eight firings of the ESEX arcjet, the radiometer placed near the thruster exit, with a view of both the arcjet plume and body, shows material degradation of the sensor thermal coating from the arcjet firings. The TQCM sensor located adjacent to this radiometer observed a slight mass loss during arcjet firing,[3] presumably due to vaporization of previously collected material or chemical interaction with plume exhaust species. Radiometers with no view of the arcjet, or a view of only the plume, show no measurable degradation. Thus, although some degradation is associated with thruster firing, the effect is observed only on sensors placed very near and with a direct view of the exhaust nozzle of the thruster. It is highly unlikely that critical materials or sensors would be located this close to the thrusters exit plane in an operational high-power electric propulsion

Received 22 January 2001; revision received 18 June 2001; accepted for publication 4 February 2002.

*Project Scientist, Propulsion Directorate, AFRL/PRSS, 1 Ara Road. Member AIAA.
†Project Engineer, 1 Ara Road; currently Chief Scientist, W. E. Research, 4360 San Juan Court, Rosamond, CA 93560. Member AIAA.
‡Electric Propulsion Space Experiment Program Manager, Propulsion Directorate, AFRL/PRSS, 1 Ara Road. Member AIAA.
§Electric Propulsion Space Experiment Chief Scientist; currently Research Scientist, Jet Propulsion Laboratory, Mail Stop 125-109, 4800 Oak Grove Drive, California Institute of Technology, Pasadena, CA 91109.

system. Contamination sensors located in the backplane of the arcjet show no deleterious effects. For future programs, although engineering measures may be needed for spacecraft equipment in the immediate vicinity of the thruster body, the arcjet environment is generally benign.

II. Onboard Radiometer Sensors

The ESEX flight unit is equipped with four microbalances, four radiometers, and two sections of GaAs solar array cells. The sensors are positioned on the ESEX flight unit as shown in Fig. 1 and Ref. 4. Specific radiometer sensor locations are listed in Table 1. In Table 1, an angle equal to 0 deg is defined as horizontal with respect to the thruster exit plane, with negative values in the backflow region. When the sensor angle is equal to 90 deg, the sensor normal is directed toward the center point of the thruster exit plane. Radiometer 1 is located on the diagnostic tower adjacent to TQCM 1, where it has a direct view of the arcjet body and plume. Radiometers 2 and 4 have a view of the arcjet plume, but are blocked from arcjet body emission by the thermal shield. Radiometer 3 on the diagnostic deck has no direct view of either the arcjet body or plume.

The radiometers, shown schematically in Fig. 2, consist of titanium witness plates 32 mm in diameter supported by a 9.5-mm-diam, 2.4-mm-long titanium strut and an insulating nylon bushing. The titanium strut, with a thermal conductivity of 1.8 W/cm · K, is the dominant heat path between the witness plate and the base of the sensor. A reflective aluminum housing surrounds the entire assembly except for the front face of the witness plate. The temperature of the witness plate and base are measured using thermocouples with an accuracy of ±1 K. These temperature measurements are used to calculate the heat flux through the radiometer assembly according to

Table 1 Locations of radiometer sensors relative to arcjet exhaust plane

Radiometer no.	Distance, cm	Position angle, degrees	Sensor face angle, deg
1	40	−11	79
2	48	−37	53
3	45	−60	60
4	60	−41	41

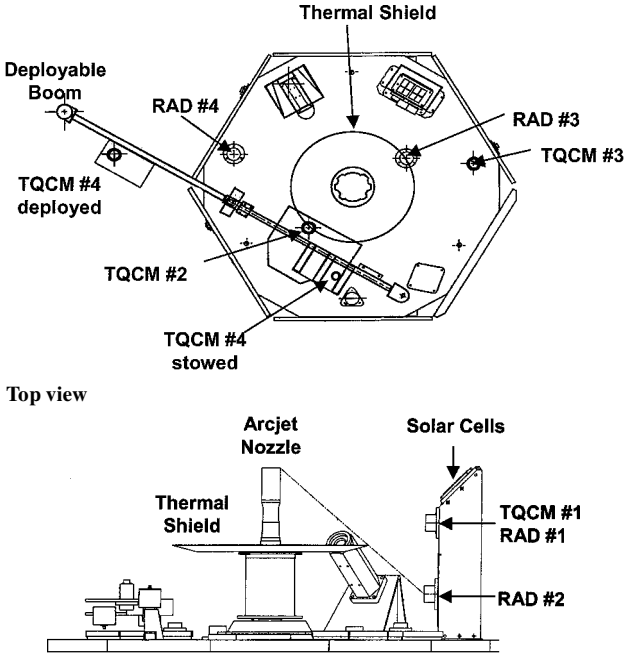

Fig. 1 ESEX showing the locations of the contamination sensors.

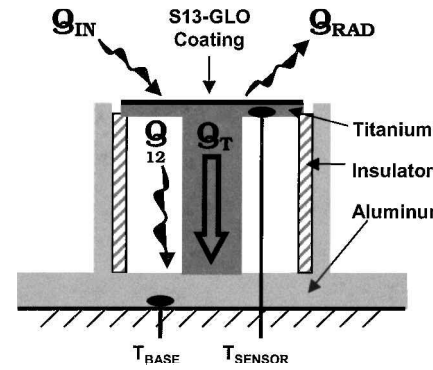

Fig. 2 Schematic diagram of the ESEX radiometers, radiometer base is 7.4 cm in diameter.

$$\dot{Q}_{\text{in}} = \dot{Q}_{\text{rad}} + \dot{Q}_{12} + kA\frac{\mathrm{d}T}{\mathrm{d}x} + mC_P\frac{\mathrm{d}T}{\mathrm{d}t}$$

where the incident radiative heat flux $\dot{Q}_{\text{in}}$ is predominantly due to solar radiation and emission from the firing arcjet. Once the system has reached thermal equilibrium, the temperature difference between the sensor face and the radiometer base, ΔT, corresponds to the net heat flux at the sensor face. This is dominated by infrared (IR) graybody emissivity ($\dot{Q}_{\text{rad}}$) and, when in sunlight, by solar absorbtivity ($\dot{Q}_{\text{in}}$). Thus, the eclipse or shadow temperature difference between sensor head and base corresponds directly to the IR emissivity of the face and, with this emissivity known, measurements in sunlight can be used to determine solar absorptivity. To calculate the heat flux from the measured radiometer temperatures, typically 10 data points are used from equivalent times in sequential orbital solar cycles. This statistically reduces the ±1 K measurement uncertainity to ±0.3 K. Calculations of heat flux will have a proportional accuracy. For typical radiometer temperature differences of 5 K, the uncertainty in the calculated heat flux is 8%

The radiometer face is coated with an approximately 0.005-in-(0.13-mm-) thick coating of S13-GLO white paint with a nominal emissivity of approximately 0.25 in the visible range, increasing to 0.85 in the IR. This is a commonly used coating for spacecraft thermal control, but is known to degrade due to solar UV and charged particle interactions, which causes changes in the emissivity and generally larger changes in the absorbtivity. The degradation of the coating in response to the emission spectrum of the 30-kW arcjet is not known, but is investigated as part of the ESEX flight experiment.

The radiometer transient thermal response is dependent on several factors, including sensor design, thermal path to the host spacecraft, and the incident solar radiation during the orbit cycles. Ideally, a full characterization and modeling of the thermal environment would be performed to fully analyze the flight radiometer data. Unfortunately, the development of a validated thermal model of the radiometer attached to the ARGOS spacecraft was not pursued due to programmatic limitations. Instead, limited ground testing[6] coupled with on-orbit exposure to the known solar flux provides the radiometer calibration. Radiometer ground tests without the sensor attached to the spacecraft and with the sensor exposed to a constant heat source show a $1/e$ time response of 15 min. At the beginning of the ARGOS flight, and before any arcjet firings, the radiometers measure $\Delta T = 5.0 \pm 0.4$ K at the peak of the solar cycle, when they have been exposed to near-normal solar flux for long enough to approach equilibrium. With the solar flux at the ARGOS orbit of 1358 W/m^2 and the initial solar absorbtivity of the S-13GLO paint of 0.25, this gives a radiometer calibration of 70.0 ± 5.6 W/m^2 · K.

III. Flight Data

The ARGOS host spacecraft for ESEX was launched 23 February 1999 from Vandenberg Air Force Base using a Delta II launcher into a 97-deg, sun-synchronous orbit at 846-km altitude. The ESEX contamination diagnostics were powered up to collect data 1 h, 25 min after launch. A total of eight ESEX firings were performed between 15 March 1999 and 21 April 1999. Following the eighth firing, a battery anomaly occurred, which precluded additional firings. The

Table 2 Contamination events during ESEX flight experiment

Firing (F) or event	Date/Time (zulu)	Julian date	Duration
Boom deployed	9 March 1999 14:59:57	68.62497	
F-1C	15 March 1999 21:55:55	74.91383	2 m, 21 s
F-2	19 March 1999 22:32:23	78.93916	5 m, 1 s
F-3	21 March 1999 12:24:41	80.51714	5 m, 33 s
F-4	23 March 1999 21:27:57	82.89441	8 m, 2 s
F-5	26 March 1999 12:45:25	85.53154	6 m, 4 s
F-6	31 March 1999 13:05:37	90.54557	4 m, 29 s
F-7	2 April 1999 22:09:03	92.92295	53 s 38 s
F-8	21 April 1999 12:22:12	111.51542	42 s
Battery anomaly	22 April 1999 15:18:37	112.63793	

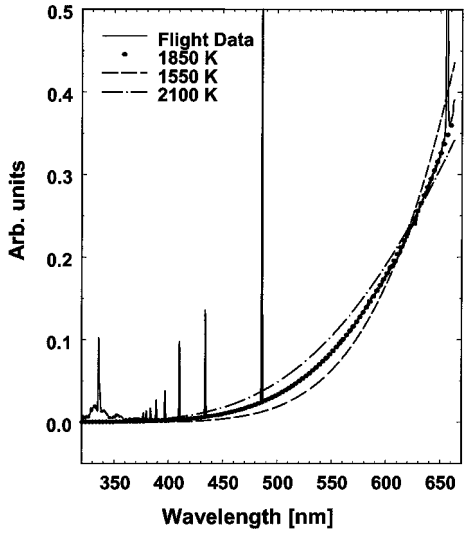

Fig. 3 Arcjet emission spectrum measured in flight is comparable to a 1850-K graybody emitter.

ESEX events, including the battery anomaly are described in detail in Ref. 1. A summary of the ESEX events related to the contamination measurements is shown in Table 2. The arcjet onorbit emission spectra[6] is shown in Fig. 3. The emission is comparable to an 1850 K graybody emitter.

Figures 4 and 5 show the sensor and base temperatures for radiometer 1 during the period surrounding firing 4. At eight minutes, firing 4 was the longest of the ESEX experiment. Figure 4 shows the radiometer temperatures oscillating with the solar cycle as ARGOS orbits. Figure 5 shows the same data on an expanded time base to illustrate the details of the radiometer response to the arcjet firing. Both the base and sensor temperatures are observed to rise through the firing, never achieving a thermal equilibrium. Other observations, particularly video images[7] and solar cell measurements, indicate that radiant emissions from the arcjet remain nearly constant after the first 2 or 3 min of operation. The arcjet itself also reaches thermal equilibrium in that period.[8] Therefore, the lack of thermal equilibrium in the radiometer signal is attributable soley to the 15-min response time of the sensor, rather than a nonequilibrium thermal emission from the arcjet source.

The radiometers do maintain near-equilibrium conditions during the much slower variations in solar illumination during the ARGOS orbit period, aside from the transient behavior as the spacecraft enters and leaves eclipse. This allows a determination of the heat absorbed by the radiometers over the course of the solar cycle.

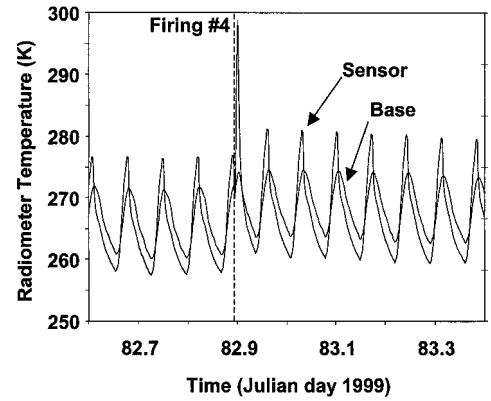

Fig. 4 Radiometer 1 sensor face and base temperature response over several orbit periods: vertical dashed line denotes time of firing 4.

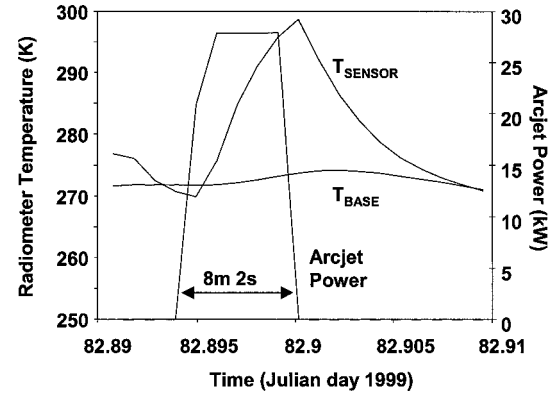

Fig. 5 Radiometer 1 response during arcjet firing 4.

Because solar illumination as a function of orbit phase is known and repeatable, this provides a measurement of the solar absorbtivity and IR emissivity of the radiometer surface coating and enables the detection of changes in these properties as a result of firing the arcjet. As seen in Fig. 4, the behavior of the radiometers over the solar cycle is consistently repeatable before the arcjet firing. After the arcjet firing, the long-term behavior is again consistently repeatable, but the average temperature of the sensor head and base has increased by several degrees. The temperature difference between the radiometer sensor face and base under solar illumination also increases, indicative of a change in the coating, whereas the temperature difference in shadow remains relatively constant. An overall increase in both sensor and base temperature is also observed after the firing and decays back to the prefiring levels over about 10 orbits, consistent with heat flux from the arcjet causing localized heating that decays on the slower thermal response time of the spacecraft.

Figure 6 shows the behavior of the radiometers throughout the mission, with the arcjet firings indicated for reference. The heat flux calculated from radiometer sensor head and base temperatures are plotted at the point of maximum incident solar flux during the orbit period, corresponding quite closely to the maximum observed heat flux in the radiometers, as expected for a system at or close to thermal equilibrium. Again, we see an increased heat flux associated with the arcjet firings.

Radiometer 1, with close, direct exposure to the arcjet plume and body, shows the most dramatic effect. Before the arcjet firings, radiometer 1 measures a fairly constant 0.27 ± 0.02 W heat load at maximum incident solar flux. With the onset of arcjet activity, this value shows a steady rise, reaching a value of 0.36 ± 0.03 W after seven arcjet firings totaling 33 min of operation. This suggests a corresponding increase in the solar absorbtivity of the surface coating of the radiometer. Another, smaller increase, to 0.39 ± 0.03 W, is observed following the battery anomaly on day 114. The mass deposition sensor located adjacent to radiometer 1 also shows an effect coincident with arcjet firing. The collected mass is observed

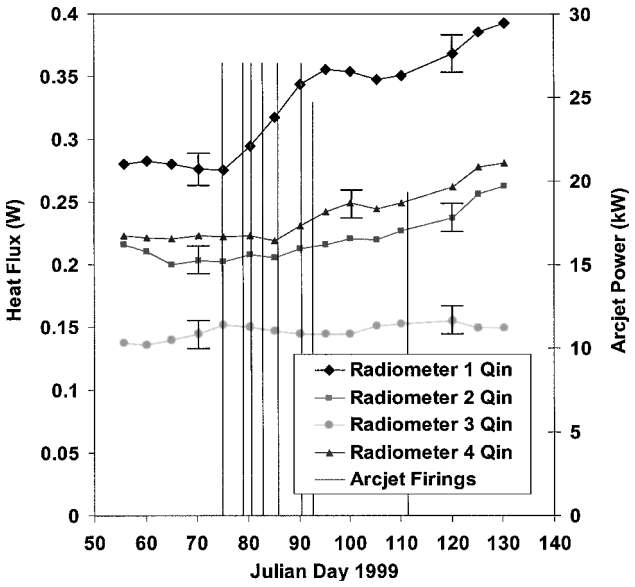

Fig. 6 Peak heat flux measured at each of the four radiometers over the duration of the ESEX flight experiment: vertical lines denote times and power levels of the eight arcjet firings.

to decrease during the firing, indicating that the arcjet has the effect of removing material from the sensor face presumably through vaporization or induced chemical reactions.[3]

Radiometers 2 and 4 exhibit similar behavior, but to a much smaller degree. Because these radiometers are shielded from arcjet body radiation, and see the plume from a greater distance than does radiometer 1, this is unsurprising. Radiometer 3, completely shielded from the arcjet, shows no significant change in heat flux or surface properties. None of the radiometers show any noticeable change in heat flux during the eclipsed portion of the orbit, suggesting that the IR emissivity of the surface coating does not change.

IV. Discussion

The rise in sensor head temperature during arcjet firing indicates that the radiometer is receiving a substantial radiated heat load from the arcjet. Figure 5 shows a temperature difference between sensor head and sensor base of 24.0 ± 0.4 K for radiometer 1 after the arcjet has fired for eight min. This indicates an absorbed heat flux of 1680 ± 133 W/m^2. However, the radiometer has clearly not reached equilibrium during the 8-min firing. Correcting for the time response of the sensor, based on the ground-test data that show an isolated radiometer exposed to heat flux of this magnitude will each 80% of its equilibrium value in 8 min, results in a corrected heat flux at the radiometer of 2100 ± 168 W/m^2.

The changes in radiometer behavior, especially that of radiometer 1, suggest a permanent change in the surface properties of the S13-GLO coating as a result of exposure to arcjet plume and body radiation. The observed heat flux during periods when the radiometers are in shadow does not change. Because radiometer behavior in shadow is dominated by IR emission, we conclude that the IR emissivity of the S13-GLO coating is not significantly changed. However, the 30% increase in heat flux at maximum solar illumination is significant and indicates an increase in the solar absorbtivity of the surface. This is consistent with the darkening of the white paint due to the 2100 W/m^2 radiation flux from the arcjet body. Radiometers shielded from the arcjet body exhibit much smaller changes in absorbtivity, even though exposure to the plume exhaust species is comparable to that of radiometer 1. This argues against plume chemistry or radiation being responsible for the degradation.

V. Summary

An analysis of radiometer data from the ESEX flight is performed to explore the contamination and/or degradation of a typical spacecraft thermal coating in response to the emission spectra associated with the use of the 30-kW arcjet. Radiometer data at four locations on the spacecraft indicate material degradation of the S13-GLO coating only for the radiometer nearest the arcjet nozzle with a full view of the exhaust plume and the arcjet body. A 30% increase in heat transfer through the coating is observed following the eight arcjet firings. Radiometers obscured from the arcjet body, with a view of only the plume, showed no evidence of surface coating degradation.

In general, degradation was observed only for sensors placed very near the arcjet nozzle, much closer than would be designed on an operational spacecraft. This degradation took the form of a 30% increase in surface absorbtivity of the S13-GLO paint. Sensors showed no degradation in the thruster backplane. The ESEX data suggest that the contamination associated with the operation of high-power electric propulsion can be controlled through relatively simple design adjustments.

Acknowledgments

The authors would like to extend their gratitude for the expert technical contributions of Mary Kriebel, Don Baxter, Bob Tobias, David Lee, David Huang, and N. John Stevens of TRW in the design and development of the flight diagnostic package. David White of W. E. Research was invaluable collecting and interpreting the raw Advanced Research Global Observation Satellite (ARGOS) telemetry data. We also acknowledge the ARGOS program office and the flight operations team at Kirtland Air Force Base for their technical expertise, as well as their insight and flexibility in the mission operations.

References

[1]Bromaghim, D. R., LeDuc, J. R., Salasovich, R. M., Spanjers, G. G., Fife, J. M., Dulligan, M. J., Schilling, J. H., White, D. C., and Johnson, L. K., "Review of the Electric Propulsion Space Experiment Program," *Journal of Propulsion and Power*, 2002.

[2]Turner, B. J., and Agardy, F. J., "The Advanced Research and Global Observation Satellite (ARGOS) Program," AIAA Paper 94-4580, Sept. 1994.

[3]Spanjers, G. G., Schilling, J. H., Engelman, S. F., Bromaghim, D. B., and Johnson, L. K., "Mass Deposition Measurements from the 26-Kilowatt Electric Propulsion Space Experiment Flight," *Journal of Propulsion and Power*, 2002.

[4]Schilling, J. H., Spanjers, G. G., Bromaghim, D. B., and Johnson, L. K., "Solar Cell Degradation During the 26-Kilowatt Electric Propulsion Space Experiment Flight," *Journal of Propulsion and Power*, 2002.

[5]Dulligan, M. J., Bromaghim, D. B., Zimmerman, J. A., Salasovich, R. M., Hardesty, D., and Johnson, L. K., "Effect of Electric Propulsion Space Experiment 26-Kilowatt Operation on Spacecraft Communications," *Journal of Propulsion and Power*, 2002.

[6]Cassady, R. J., Hoskins, W. A., Vaughan, C. E., "Qualification of a 26-kW Arcjet Flight Propulsion System," AIAA Paper 95-2505, 1995.

[7]Johnson, L. K., Spanjers, G. G., Bromaghim, D. R., Dulligan, M. J., and Hoskins, W. A., "On-Orbit Optical Observations of Electric Propulsion Space Experiment 26-Kilowatt Ammonia Arcjet," *Journal of Propulsion and Power*.

[8]Fife, J. M., Bromaghim, D. R., Chart, D. A., Hoskins, W. A., Vaughan, C. E., and Johnson, L. K., "Orbital Performance Measurements of Air Force Electric Propulsion Space Experiment Ammonia Arcjet," *Journal of Propulsion and Power*, 2002.